Review Article

Comparison of diagnostic performance between diffusion models parameters and mono-exponential apparent diffusion coefficient in patients with prostate cancer: A systematic review and meta-analysis

Hamide Nematollahi[1], Mohammad Reza Maracy[2], Masoud Moslehi[1], Daryoush Shahbazi-Gahrouei[1]

[1]Department of Medical Physics, School of Medicine, Isfahan University of Medical Sciences, Isfahan, Iran, [2]Department of Epidemiology and Biostatistics, School of Public Health, Isfahan University of Medical Sciences, Isfahan, Iran

Background: The importance of diffusion in prostate cancer (PCa) diagnosis has been widely proven. Several studies investigated diffusion models in PCa diagnosis. **Materials and Methods:** This systematic review and meta-analysis study was performed to evaluate the ability of three diffusion models to diagnose PCa from the scientific electronic databases Embase, PubMed, Scopus, and Web of Science (ISI) for the period up to March 2022 to identify all relevant articles. **Results:** Eighteen studies were included in the systematic review section (7 diffusion kurtosis imaging [DKI] studies, 4 diffusion tensor imaging [DTI] studies, 4 intravoxel incoherent motion [IVIM] studies, and 3 IVIM-DKI studies). Pooled sensitivity, specificity, accuracy, and summary area under each diffusion model's curve (AUC) and 95% confidence intervals (CIs) were calculated. The pooled accuracy and 95% CI on detection (differentiation of tumor from normal tissue and benign prostatic hyperplasia/prostatitis) were obtained for apparent diffusion coefficient (ADC) at 87.97% (84.56%–91.38%) for DKI parameters (Gaussian diffusion [DK] 87.94% [78.71%–97.16%] and deviation from Gaussian diffusion [K] 86.84% [81.83%–91.85%]) and IVIM parameters (true molecular diffusion [DIVIM] 81.73% [72.54%–90.91%], perfusion-related diffusion [D*] 65% [48.47%–81.53%] and perfusion fraction [f] 80.36% [64.23%–96.48%]). The AUC values and 95% CI in the detection of PCa were obtained for ADC at 0.95 (0.92–0.97), for DKI parameters (DK 0.94 [0.89–0.99] and K 0.93 [0.90–0.96]) and for IVIM parameters (DIVIM 0.85 [0.80–0.91], D* 0.60 [0.43–0.77] and f 0.73 [0.63–0.84]). Two studies showed that the DTI accuracy values were 97.34% and 85%. For IVIM–kurtosis model in PCa detection, two studies stated that the DIVIM-K and KIVIM-K accuracy values were 85% and 84.44% (the pooled accuracy; 84.64% with 95% CI 75.78%–93.50%), and 72.50% and 71.11% (the pooled accuracy, 72.10% with 95% CI 64.73%–79.48%), respectively. **Conclusion:** Our findings showed that among the DKI, IVIM, and ADC parameters, it seems that ADC, Dk, DIVIM, and K are the most important, which can be used as an indicator to distinguish PCa from normal tissue. The DKI model probably has a higher ability to detect PCa from normal tissue than the IVIM model. DKI probably has the same diagnostic performance in PCa detection and grading compared to diffusion-weighted imaging and ADC.

Key words: Accuracy, area under curve, diffusion kurtosis imaging, diffusion tensor imaging, diffusion-weighted imaging, intravoxel incoherent motion, multiparametric magnetic resonance imaging

How to cite this article: Nematollahi H, Maracy MR, Moslehi M, Shahbazi-Gahrouei D. Comparison of diagnostic performance between diffusion models parameters and mono-exponential apparent diffusion coefficient in patients with prostate cancer: A systematic review and meta-analysis. J Res Med Sci 2024;29:43.

INTRODUCTION

Prostate cancer (PCa) is the most common cancer in males and the second leading cause of death from cancer.[1] Commonly used methods for screening (diagnosing) PCa include prostate-specific antigen (PSA) test, digital rectal examination, and transrectal ultrasound-guided prostate biopsy. These methods are invasiveness or have

Access this article online

Quick Response Code:

Website: https://journals.lww.com/jrms

DOI: 10.4103/jrms.jrms_359_23

Address for correspondence: Prof. Daryoush Shahbazi-Gahrouei, Department of Medical Physics, School of Medicine, Isfahan University of Medical Sciences, Isfahan, Iran.
E-mail: shahbazi@med.mui.ac.ir

Submitted: 03-Jun-2023; **Revised:** 05-Aug-2023; **Accepted:** 12-Feb-2024; **Published:** 30-Jul-2024

low accuracy.[2-5] Specific urinary biomarkers related to PCa are also reported, although confirming these biomarkers requires significant research.[6]

In recent years, various studies have shown the role of multiparametric magnetic resonance imaging (mpMRI) for the detection and assessment of aggressiveness of PCa (with high sensitivity and specificity).[4,7,8] The mp-MRI is known as the combination of conventional anatomical (T1- or T2-weighted imaging) and at least two functional MRI techniques: dynamic contrast-enhanced MRI (DCE-MRI), diffusion-weighted imaging (DWI), and MR spectroscopy.[9,10]

DWI is a method without the use of contrast agents. Beyond conventional apparent diffusion coefficient (ADC) mapping, advanced DWI models such as intravoxel incoherent motion (IVIM), non-Gaussian diffusion MRI, and diffusion tensor imaging (DTI) are extensively used in the detection or characterization of PCa.

IVIM MRI evaluates both tissue diffusivity and tissue microcapillary perfusion at once. IVIM parameters D, D*, and f represent true molecular diffusion, perfusion-related diffusion, and perfusion fraction, respectively.[11] Diffusion kurtosis imaging (DKI) is based on non-Gaussian water diffusion. DKI parameters such as D and K represent Gaussian diffusion and deviation from Gaussian diffusion, respectively.[12,13]

The IVIM-kurtosis model simultaneously contains molecular diffusion, perfusion, and non-Gaussian information.[14]

DTI contains quantitative information on the directional diffusivity of water molecules in biological tissues. DTI can provide the mean diffusivity (MD) or ADC of water in tissues, fractional anisotropy (FA) values, and diffusion tensor tractography.[11,15]

Therefore, different MRI imaging techniques are used to detect and characterize PCa, but each has one or more limitations.[16] It can be helpful to comprehensively understand which anatomic and functional MRI sequences are more accurate and sensitive than others in detecting and characterizing PCa. Ultimately, the optimal combination of anatomic and functional MRI sequences for detecting and characterizing PCa is necessary. According to our knowledge, no systematic review studies have been performed to determine the diagnostic performance of the three MRI diffusion models (DKI, DTI, and IVIM) and the IVIM-Kurtosis model compared to ADC in detecting or predicting the grade of PCa.

This systematic review and meta-analysis aimed to determine the accuracy of each diffusion model compared to ADC in diagnosing PCa.

METHODS

This systematic review and meta-analysis were done under the Preferred Reporting Items for Systematic Reviews and Meta-analyses (PRISMA) statement.[17]

Search strategy

We systematically searched the scientific electronic databases Embase, PubMed, Scopus, and Web of Science (ISI) for the period up to March 2022 to identify all relevant articles. The search strategy included the combination of the following keywords: (prostate OR prostatic) AND (cancer OR tumor OR carcinoma OR neoplasm) AND ("magnetic resonance imaging" OR MRI OR MR) AND ("diffusion tensor imaging" OR DTI OR "diffusion kurtosis imaging" OR DKI OR "intravoxel incoherent motion" OR IVIM) AND (sensitivity OR specificity OR accuracy).

The literature search was restricted to English-language articles except for review articles.

Eligibility criteria and study selection

The two reviewers (individually) checked the titles and abstracts of the identified articles. Then, the two reviewers independently assessed the eligibility by reading the articles. The full text of the evaluated articles was considered with at least one diffusion model (DKI, DTI, and IVIM) to detect or characterize PCa.

In reviewing the full text of the articles, articles that mentioned sensitivity, specificity, and/or accuracy for diffusion models were selected. The exclusion criteria were: (1) the full text of the articles without the English language, (2) radiomic studies, and (3) studies without sufficient report data.

The PRISMA flow diagram of considered studies by the inclusion and exclusion criteria is summarized in Figure 1.

Data extraction

Data extraction was performed independently by two authors. The data that were extracted: study author, year of publication, study country, study design, reference standard, number of patients, number of regions, patient age, PSA level, Gleason score (GS) range, magnetic field strength, anatomic zone evaluated, b values, type of coil, blinding, number of readers, slice thickness, sensitivity value, specificity value, and accuracy value.

Quality assessment

Quality assessment of the included studies was performed using two independent reviewers using the Quality Assessment Tool for Observational Cohort and Cross-Sectional Studies (NHLBI). The cross-sectional and

cohort tool consists of 14 questions and the case–control tool contains 12 questions, each scoring 0 or 1, to determine the potential flaws in study methods or implementation. Judgments on the overall methodological quality will be determined by the total score for each article as follows: low quality (≤50% of overall score), moderate quality (50%–70% of overall score), and high quality (≥70% of overall score). A third reviewer settled any differences. (https://www.nhlbi.nih.gov/health-topics/study-quality-assessment-tools.).

Data synthesis and analysis (statistical analysis)

Data from the studies, including true and false-positive numbers and true and false-negative numbers, were collected from the eligible paper to determine sensitivity, specificity, accuracy, and corresponding 95% confidence intervals (CIs) using forest plots. In addition, to validate the diagnostic tests, we used the receivers' operating characteristic (ROC) curves. Random-effects restricted maximum likelihood was used to run the models. An $I^2 > 50\%$ and a $P < 0.05$ indicated substantial heterogeneity. Galbraith plot was carried out to assess the sources of heterogeneity among studies. Subgroup analysis was performed using DKI (D and K) and IVIM (D, D*, f). Funnel plot, Egger, and Begg tests were utilized to assess publication bias. A nonparametric trim-and-fill analysis of publication bias was utilized to evaluate the number of missing studies. All data analyses were calculated using Stata software version 16 (StataCorp LLC 4905 Lakeway Drive College Station, Texas 77845-4512. USA) and RevMan (version 5.3, The Cochrane Collaboration).

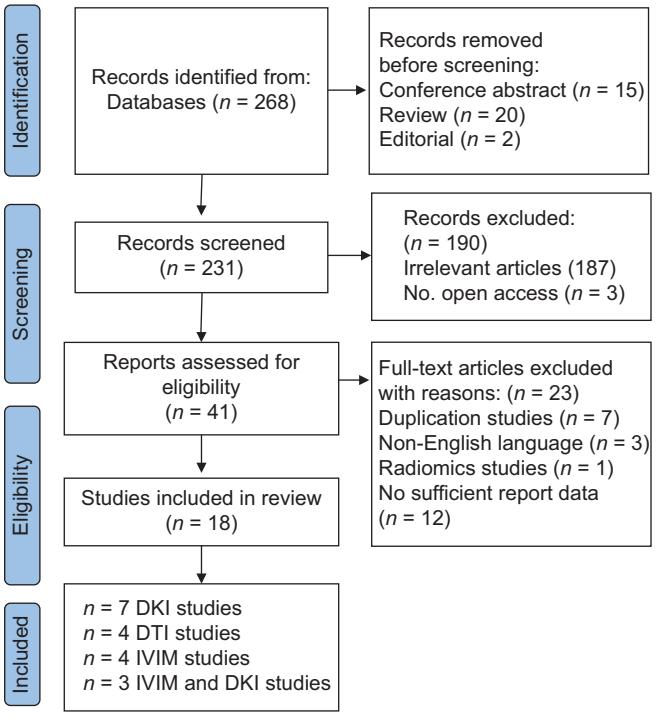

Figure 1: Preferred Reporting Items for Systematic Reviews and Meta-analyses 2020 flow diagram for systematic reviews. DKI: Diffusion Kurtosis Imaging, DTI: Diffusion Tensor Imaging, IVIM: Intravoxel Incoherent Motion model

RESULTS

As mentioned before, the paper acquisition is reported in Figure 1. The results of the quality assessment are shown in Figure 2. Figures 3-5 show forest plots of accuracy for each diagnostic modality. 18 of 268 studies remained for inclusion in our systematic review. Table 1 shows the study and patient characteristics of the included studies. Tables 2 and 3 report methodologic and MRI protocol characteristics and measurement of diagnostic performance among diffusion models of included studies, respectively.

Results of qualitative analysis

Studies on apparent diffusion coefficient

Most of the studies, along with IVIM and DKI parameters, reported the value of ADC in tumor tissue and normal tissue or benign prostatic hyperplasia (BPH)/prostatitis. Most studies showed a significantly lower ADC value in tumor tissue than in normal tissue and BPH/prostatitis, with an increasing tendency in high GS lesions.[14,19-24,26]

Studies on diffusion kurtosis imaging

The number of 10 out of 18 studies involving 875 patients reported the diagnostic performance of DKI parameters. Of these, eight were on detection (differentiation of tumor from normal tissue and BPH/prostatitis),[14,18-22,24,25] two on characterization (The meaning of the studies that have mentioned the accuracy of distinguishing low-grade tumors from intermediate-high grade tumors),[23,26] and two on both.[21,24]

In all selected studies, the K and D values were useful for discriminating both PCa from normal tissue/BPH/prostatitis and low from high GS tumors. Studies have reported that the K and D values were significantly higher and lower in the

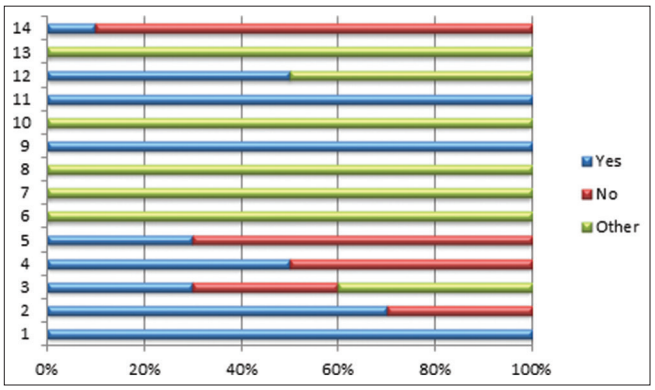

Figure 2: The result of quality assessment. One score was given to the question with a Yes answer, a zero score to answer No, and a no score to other answer (Cannot determine, Not applicable, and Not report). In the end, the scoring average of all articles was received at 71.39%

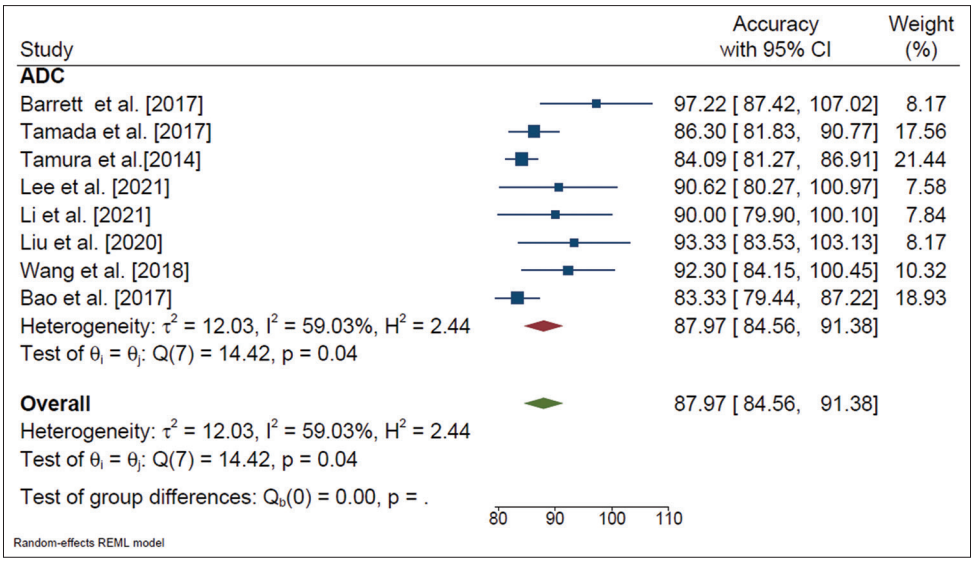

Figure 3: The forest plot of apparent diffusion coefficient in detecting prostate cancer (differentiation of tumor from normal tissue and benign prostatic hyperplasia/prostatitis)

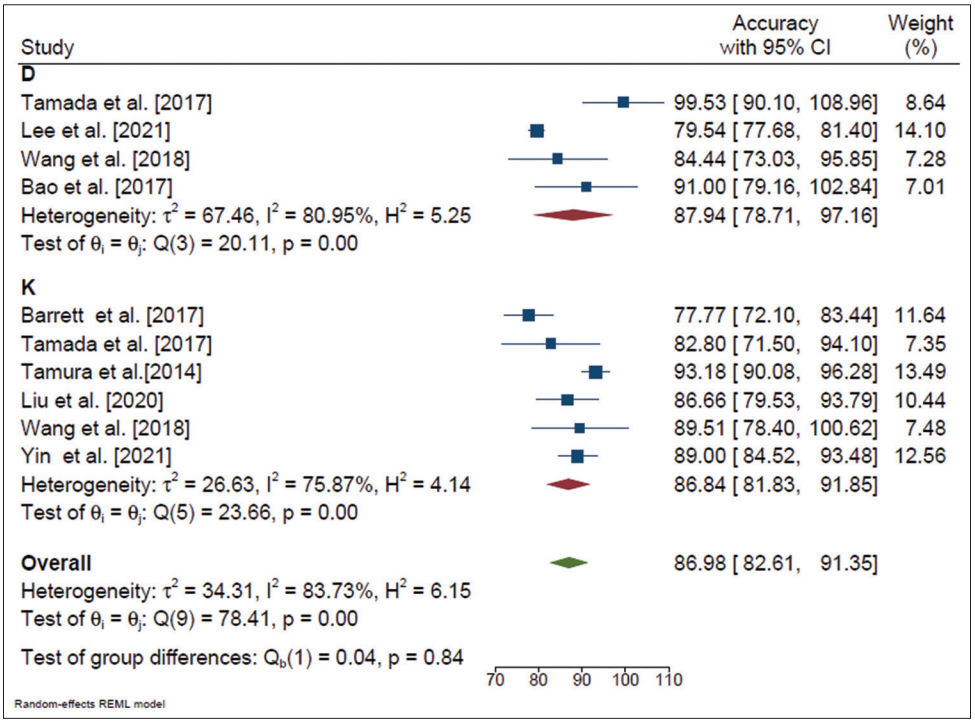

Figure 4: The forest plot of diffusion kurtosis imaging parameters in detecting prostate cancer (differentiation of tumor from normal tissue and benign prostatic hyperplasia/prostatitis)

tumors than in normal tissue/BPH/prostatitis[14,19,21,22,24,25] and in high-GS tumors than in low-GS tumors,[21,23-26] respectively.

The opinions (results) of several studies about the better ability of DKI over ADC were like this.

Park *et al*. concluded that the DKI parameters have a diagnostic performance comparable to mono-exponential ADC in diagnosing patients with high- and low-grade PCa.[26] Wang *et al*. found that the AUCs of Kapp are significantly lower than the AUCs ADC in the diagnosis and grading of PCa.[24] Tamada *et al*. reported that ADC and K had similar diagnostic performances. Also, compared to DWI, DKI did not have a clear added value for the clinical evaluation of PCa.[21] Liu *et al*. stated that the mono-exponential and kurtosis models have the same diagnostic efficiency in diagnosing PCa.[14] In the end, Barrett *et al*. found that ADC, Dapp, and Kapp distinguished tumors from benign tissue, but none reliably discriminated between high-grade and low-grade tumors.[19]

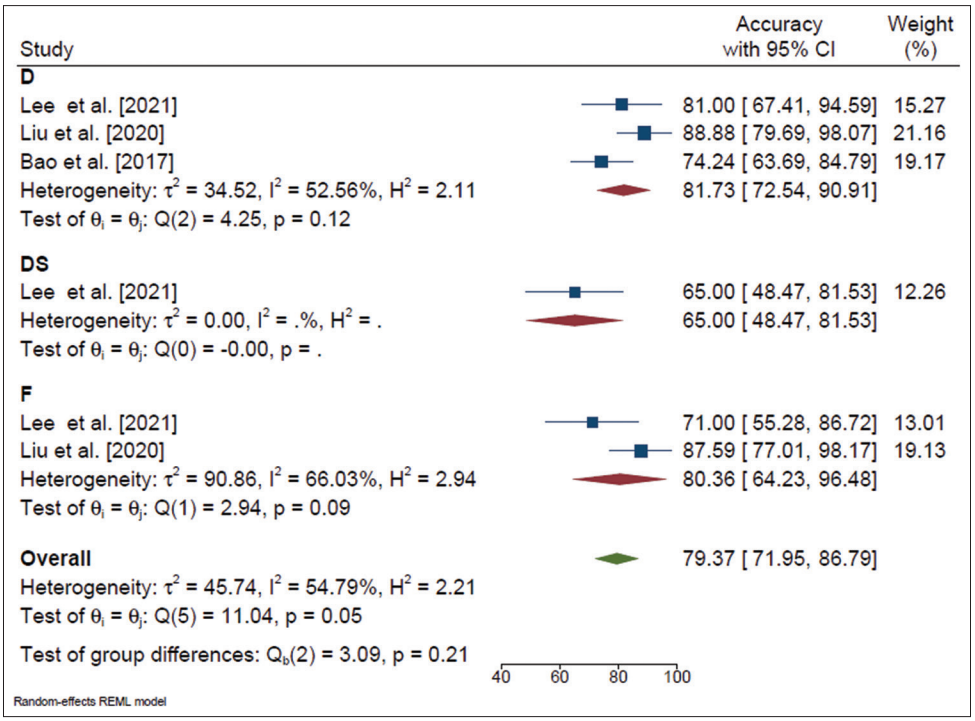

Figure 5: The forest plot of intravoxel incoherent motion parameters in detecting prostate cancer (differentiation of tumor from normal tissue and benign prostatic hyperplasia/prostatitis)

For the relationship between DKI parameters and GS, the results mentioned by the articles are as follows. Neither D nor K parameters reliably separate high-grade and low-grade tumors. There is a nonsignificant negative correlation between the parameters of K and D with GS. K significantly differs between low- and moderate-grade and moderate- and high-grade tumors. Tumors with high grades significantly have a lower average D and higher K compared to low grades.

Studies on diffusion tensor imaging

The number of 4 of 18 studies involving 108 patients reported the diagnostic performance of DTI.[27-30] Chen *et al*. stated that there is a significant negative correlation between GSs and MD values. They determined the optimum MD threshold of 1.0×10^{-3} mm²/ms.[27] Kozlowski *et al*. showed that DTI parameters (FA and MD) significantly differed between the tumor and normal tissue in the peripheral zone (PZ) and the whole prostate. However, only for MD, there was a significant difference between the tumor and normal tissue in the transition zone (TZ). The AUCs FA in the whole prostate was significantly lower than the AUCs MD. However, there were no significant differences between the AUC values in PZ.[28]

In another study, Kozlowski *et al*. showed that the value of AUC related to MD is significantly higher than that of FA. On the other hand, the value of AUC related to FA was such that they stated that this parameter alone is not helpful in diagnosing the tumor and normal PZ.[29] Li *et al*. demonstrated significant differences in the ADC and FA values between cancerous and noncancerous tissue in PZ.[30]

It is also helpful to mention that in most of these studies, a comparison was made between DTI and quantitative DCE. Two studies stated that the AUC for DTI + DCE parameters was significantly higher than that for either DTI or DCE parameters alone.[29,30] A study showed that DTI + DCE and DTI parameters operate superior to DCE parameters alone. However, the AUC value for DTI + DCE parameters was not significantly different from the AUC value for DTI parameters alone.[28]

Studies on intravoxel incoherent motion

The number of 7 of 18 studies involving 356 patients reported the diagnostic performance of the IVIM parameters. Of these, six were on detection (differentiation of tumor from normal tissue and BPH/prostatitis), and one was on characterization.

Two studies on distinguishing cancerous tissue from normal tissue found that D was significantly smaller in PCa than in normal tissue.[33,34] Valerio *et al*. stated that D* was significantly higher in PCa than in normal tissue.[34] However, Lee *et al*. stated that D* and f parameters values were insignificant between these two tissues.[33] Liu *et al*., regarding the diagnosis of PCa from BHP, stated that D and f are significantly lower in PCa compared to BHP.[14] However, Bao *et al*. concluded that D is significantly lower in PCa than BHP, but f and D* were not significantly different.[31]

Table 1: Study and patient characteristics of included studies

Author (year)	Country	Study design	Reference standard	Number of patients	Number of regions or lesions	Number of positive regions	Number of patients with PCa	Parameter	Age/age range	PSA/PSA range	Gleason score range	Anatomic zone evaluated	Blinding
Akamine *et al.* (2020)[18]	Japan	Retrospectively	Radical prostatectomy	52	126	63	52	DKI-IVIM	64.9 - mean/50–76	8.63 - mean/2.46–18.2		TZ and PZ	NR
Barrett *et al.* (2018)[19]	UK	Prospectively	Biopsy	30	36	26	24	DKI	65.50 - median/50–76	7.67 - median/6.12–11.98	6–≥8	TZ and PZ	NR
Li *et al.* (2021)[20]	China		Biopsy	30	40	20		DKI-IVIM	72 - mean/64–80	18.84 - mean/0.99–36.69			Blind to the pathological result
Liu *et al.* (2020)[14]	China	Prospectively	Biopsy	36	45	18	16	DKI-IVIM	74.38±7.99	15.82± 15.60	6–9		NR
Tamada *et al.* (2017)[21]	Japan	Retrospectively	Radical prostatectomy	285			285	DKI	NR	NR	6–≥8	TZ and PZ	NR
Tamura *et al.* (2014)[22]	Japan	Retrospectively	Radical prostatectomy	20	85	24	20	DKI	66.4±6.1 - mean/52–75	8.48±5.2 - mean/3.49–21.52	6–9		Blind
Wang *et al.* (2015)[23]	China	Retrospectively	Radical prostatectomy	110	126	126	110	DKI	69.5 - median/48–86	12.1 - median/1.5–656.0	6–≥8	TZ and PZ	NR
Wang *et al.* (2018)[24]	China	Retrospectively	Biopsy	120	143	90	67	DKI	72.7 - median/53–90	10.1/1.0–656.0	≤6–≥8	TZ and PZ	Blind
Yin *et al.* (2021)[25]	China	-	Radical prostatectomy or biopsy	100			49	DKI	72.86±7.23		<7–10		Blind
Park *et al.* (2020)[26]	Korea	Retrospectively	Radical prostatectomy or biopsy	92			92	DKI	71.5 - mean/47–89	139.6103 - mean/0.03–4484	6–10	TZ and PZ	Blind to the pathological result
Chen *et al.* (2011)[27]	Taiwan		Biopsy	37			37	DTI	63 - mean/55–72	7.8 - mean/4–20		PZ	Blind
Kozlowski *et al.* (2018)[28]	Canada	–	Radical prostatectomy	16	191	64	16	DTI	62.4 - mean/50–69	6.5 - mean/2.6–11.4	6–7	TZ and PZ and entire pro	NR
Kozlowski *et al.* (2010)[29]	Canada	Prospectively	Biopsy	22			10	DTI	62.5 - mean/55–72	6.8/5.3–12	6–9	PZ and CG	NR
Li *et al.* (2014)[30]	China	Retrospectively	Biopsy	33	198	62	16	DTI	66± 10 - mean/42–82	8.7 - mean/4.2–50.9	6–9	PZ	Blind to the pathological result
Bao *et al.* (2017)[31]	China	Prospectively	Biopsy	63			30	IVIM	69± 1.54 mean	72.13±26.93 - mean	6–10	TZ	NR
Barbieri *et al.* (2017)[32]	Switzerland	Prospectively	Radical prostatectomy	84			84	IVIM	64 - median/43–80	NR	6–10		Blind
Lee *et al.* (2021)[33]	Taiwan		Radical prostatectomy	38			16	IVIM	68.1 - mean/50–84	9.62 - mean/3.38–22.68	7–9	PZ and TZ	NR
Valerio *et al.* (2016)[34]	Italy	Prospectively	Biopsy	53			53	IVIM				PZ	Blind

PCa=Prostate cancer; TZ=Transition zone; PZ=Peripheral zone; NR=Not report; IVIM=Intravoxel incoherent motion; DTI=Diffusion tensor imaging; DKI=Diffusion kurtosis imaging; PSA=Prostate-specific antigen; CG=Central gland

Table 2: Magnetic resonance imaging characteristics

Author (year)	Parameter	*b*	Field strength (*t*)	Type of coil	Use of endorectal coil	Slice thickness
Akamine *et al*. (2020)[18]	DKI-IVIM	0, 50, 100, 200, 500, 1000, 2000, 3000	3.0	Not report	Not report	3.0
Barrett *et al*. (2018)[19]	DKI	150, 450, 800, 1150, 1500	3.0	32-channel phased-array coil	No	3.6
Li *et al*. (2021)[20]	DKI-IVIM	0, 20, 50, 100, 200, 500, 1000, 1500, 2000	3.0	An 8-channel cardiac coil	No	4.0
Liu *et al*. (2020)[14]	DKI-IVIM	0,20, 50, 100, 200, 500, 1000, 1500, 2000	3.0	An 8-channel cardiac coil	No	4.0
Tamada *et al*. (2017)[21]	DKI	0, 500, 1000, 1500, 2000	3.0	An external pelvic phased-array coil	No	4.0
Tamura *et al*. (2014)[22]	DKI	0, 10, 20, 30, 50, 80, 100, 200, 400, 1000, 1500	3.0	A 16-channel phased-array coil	No	3.5
Wang *et al*. (2015)[23]	DKI	0, 700, 1400, 2100	3.0	A pelvic phased-array coil	No	3.5
Wang *et al*. (2018)[24]	DKI	200, 500, 1000, 1500, 2000	3.0	A pelvic phased-array coil (8-channel)	No	3.0
Yin *et al*. (2021)[25]	DKI	400, 800, 1200, 1600, 2000	3.0	A 32-channel phased-array torso coil	No	5.0
Park *et al*. (2020)[26]	DKI	0, 100, 1000, 2000	3.0	A parallel-array body coil (SENSE Torso/cardiac coil)	No	3.0
Chen *et al*. (2011)[27]	DTI	0, 500	1.5	-	Yes	Blind
Kozlowski *et al*. (2018)[28]	DTI	0, 600	3.0	Cardiac phased-array coil	Yes	
Kozlowski *et al*. (2010)[29]	DTI	0, 600	3.0	Cardiac phased-array coil	Yes	
Li *et al*. (2014)[30]	DTI	0, 700	3.0	An 8-channel cardiac coil	No	Blind to the pathological result
Bao *et al*. (2017)[31]	IVIM	0, 50, 100, 150, 200, 500, and 1000	3.0	A pelvic phased-array coil	No	
Barbieri *et al*. (2017)[32]	IVIM	0, 10, 20, 50, 130, 270, 500, 900	3.0	Two phased-array 8-channel coils	No	Blind
Lee *et al*. (2021)[33]	IVIM	0, 50, 100, 200, 400, 600, 1000, 1200, 1800, 2000	3.0	A 16-channel SENSE-XL-TORSO coil	No	
Valerio *et al*. (2016)[34]	IVIM	0, 10, 20, 30, 40, 50, 80, 100, 200, 400, 800	3.0	An 8-channel torso phased-array coil	Yes	Blind

IVIM=Intravoxel incoherent motion; DTI=Diffusion tensor imaging; DKI=Diffusion kurtosis imaging

For the relationship between IVIM parameters and GS, three studies reported a significant negative correlation between GS and D.[31,32,34] In addition, one of the studies reported a significant positive correlation between GS and D*.[34] Lee *et al*. found that between D, D*, and f parameters, only D* has a positive significant difference with GS.[33] Whereas Liu *et al*. found a nonsignificant negative correlation between GS and D, D* and f parameters.[14]

The opinions (results) of several studies about the superiority of IVIM over ADC were like this. Liu *et al*. concluded that the mono-exponential model (MEM), IVIM, and kurtosis were helpful in the diagnosis of PCa, and the diagnostic efficacy seemed to be similar.[14] Bao *et al*.'s study concluded that the diagnosis efficiency of IVIM parameters was not superior to ADC in diagnosing PCa in the TZ.[31] Lee *et al*. reported that the ADC parameter had the highest accuracy in differentiating PCa from normal tissue compared to IVIM parameters.[33] Barbieri *et al*. concluded that classification by IVIM parameters was not superior to that by ADC.[32]

Studies on the intravoxel incoherent motion-kurtosis model

Li *et al*. stated that the K mean value was significantly higher, and ADC and D mean values were significantly lower in PCa than in BPH/prostatitis. The mean of D and D* had a significant negative correlation with GS, whereas the mean of K and f had a significant positive correlation with GS. Finally, they concluded that the IVIM-kurtosis model has a better ability than the MEM to distinguish PCa from BPH/prostatitis. Furthermore, they stated the IVIM-kurtosis model might give more data in the grading of PCa compared with MEM.[20] Liu *et al*. concluded that the MEM, kurtosis, IVIM, and IVIM–kurtosis models probably have the same diagnostic efficacy for diagnosing PCa. Furthermore, the IVIM–kurtosis model may be superior to the MEM, kurtosis, and IVIM models in predicting GS of PCa.[14]

Results of meta-analyses

From 18 studies, a meta-analysis was performed on 16 studies. Some studies were not subjected to meta-analysis due to the lack of sufficient data.

Risk of bias

Publication bias was investigated using a funnel plot, Egger, and Begg tests. All three methods rejected publication bias. The results of this study based on Egger's test show that the beta value is −1.4, and the probability value is equal to 0.214. Furthermore, based on Begg's test, Kendal's score is −69, and the probability value (*P* value) is 0.27, both of which confirm that the effect of small studies can be ignored, and as a result, the publication bias is rejected.

Diagnostic performance of diffusion models in prostate cancer detection and grading

The forest plots of accuracy from eight studies for ADC, eight studies for DKI, and three studies for IVIM are shown in Figures 3-5. The I^2 and *P* value range were 54.79%–80.95% and 0.00–0.05, respectively. An $I^2 > 50\%$ and a $P < 0.05$ indicated substantial heterogeneity.

The diagnostic performance results of ADC, DKI, and IVIM models in the PCa detection are shown in Table 3.

The pooled accuracy and 95% CI on detection (differentiation of tumor from normal tissue and [BPH]/prostatitis) were obtained for ADC at 87.97% (84.56%–91.38%), for DKI parameters (D_K 87.94% [78.71%–97.16%], and K 86.84% [81.83%–91.85%]), and IVIM parameters (D_{IVIM} 81.73% [72.54%–90.91%], D* 65% [48.47%–81.53%], and f 80.36% [64.23%–96.48%]). The AUC values and 95% CI in the detection of PCa were obtained for ADC at 0.95 (0.92–0.97), for DKI parameters (D_K 0.94 [0.89–0.99], and K 0.93 [0.90–0.96]), and for IVIM parameters (D_{IVIM} 0.85 [0.80–0.91], D* 0.60 [0.43–0.77], and f 0.73 [0.63–0.84]). The pooled accuracy with corresponding 95% CIs in the detection PCa were 86.98% (95% CI, 82.61%–91.35%) for DKI and 79.37% (95% CI, 71.95%–86.79%) for IVIM. The pooled sensitivity and pooled specificity of ADC, DKI, and IVIM for PCa detection were (0.90 and 0.91), (0.91 and 0.82), and (0.77 and 0.81), respectively. The negative predictive value and positive predictive value of ADC, DKI, and IVIM for PCa detection were (89.38% and 85.31%), (89.05% and 92.49%), and (81.53% and 84.19%), respectively. The summary AUC values in the detection PCa were 0.94 (95% CI, 0.91–0.96) for DKI and 0.79 (95% CI, 0.71–0.87) for IVIM. The pooled accuracy of ADC, DKI, and DKI + ADC for PCa grading was 72.86% (95% CI 61.29%–84.43%), 71.41% (95% CI 67.02%–75.81%), and 72.13% (95% CI 67.04%–77.22%), respectively.

Table 3: Comparison of pooled measures of diagnostic performance among apparent diffusion coefficient, diffusion kurtosis imaging, and intravoxel incoherent motion in detecting prostate cancer (differentiation of tumor from normal tissue and benign prostatic hyperplasia/prostatitis)

Parameter	Pooled sensitivity	Pooled specificity	Pooled accuracy	Summary AUC
ADC	0.90	0.91	87.97	0.95
DKI	0.91	0.82	86.98	0.94
IVIM	0.77	0.81	79.37	0.79

ADC=Apparent diffusion coefficient; DKI=Diffusion kurtosis imaging; IVIM=Intravoxel incoherent motion; AUC=Area under curve

There was no significant difference between the estimated accuracy results of ADC and DKI. The results show that the DKI model probably has a higher ability to detect PCa from normal tissue than the IVIM model. DKI probably has the same diagnostic performance in PCa detection and grading as ADC. Two studies showed that the DTI accuracy values in PCa detection were 97.34% and 85%. For IVIM-kurtosis model in PCa detection, two studies stated that the D_{IVIM-K} and K_{IVIM-K} accuracy values were 85% and 84.44% (the pooled accuracy; 84.64% with 95% CI 75.78%–93.50%), and 72.50% and 71.11% (the pooled accuracy; 72.10% with 95% CI 64.73%–79.48%), respectively.

DISCUSSION

In recent years, many studies have been published using different diffusion models for detecting and characterizing PCa to determine their diagnostic performance. This study's goal was to reach a point of view on whether the parameters of three diffusion models (DKI, DTI, and IVIM) can compete with the ADC parameter in the detection and characteristic (classify, grading) of PCa. With our systematic review and meta-analysis, we qualitatively and quantitatively expressed the ability of each parameter to detect and grade PCa according to the data reported in the selected studies. To compare the better diagnostic performance of ADC with the parameters of the three diffusion models, only the articles that mentioned the diagnostic performance of ADC along with the three diffusion models were used.

According to studies, 70% and 30% of PCa occur in the PZ and TZ, respectively. The TZ is also the site of BPH, which can lead to urinary obstruction. Therefore, distinguishing PCa from BPH is essential to avoid unnecessary biopsies. In addition to cancer diagnosis, determining the degree of malignancy is necessary to control and treat the disease.[35] DWI seems to detect tumors in the PZ of the prostate more accurately than those in the TZ. This is because PCa in the PZ tends to exhibit higher cellularity and restricted diffusion, which DWI can detect.[36] On the other hand, as mentioned, tumors in the TZ may be more challenging to detect using DWI due to the presence of BPH nodules, which can also show restricted diffusion and mimic cancerous lesions.

In this meta-analysis, the pooled accuracy and 95% CI on detection (differentiation of tumor from normal tissue and [BPH]/prostatitis) were obtained for ADC at 87.97% (84.56%–91.38%), for DKI parameters (D_K

87.94% [78.71%–97.16%], and K 86.84% [81.83%–91.85%]), and IVIM parameters (D_{IVIM} 81.73% [72.54%–90.91%], D* 65% [48.47%–81.53%], and f 80.36% [64.23%–96.48%]). The AUC values and 95% CI in the detection of PCa were obtained for ADC at 0.95 (0.92–0.97), for DKI parameters (D_K 0.94 [0.89–0.99], and K 0.93 [0.90–0.96]), and for IVIM parameters (D_{IVIM} 0.85 [0.80–0.91], D* 0.60 [0.43–0.77], and f 0.73 [0.63–0.84]).

He *et al*., in a meta-analysis study with twenty articles, demonstrated that the AUC values for ADC, D_{IVIM}, D*, and f in the detection of PCa from noncancerous tissues were 87%, 85%, 75%, and 76%, respectively.[37] Using the results of five studies, Si and Liu obtained the AUC values in the detection of PCa 0.93 (95% CI, 0.90–0.95) for ADC, 0.89 (95% CI, 0.86–0.92) for D_K, and 0.93 (95% CI, 0.90–0.95) for K.[38] According to the selected articles in this study, it can be definitely stated that the values of ADC, D_K, and D_{IVIM} are significantly higher, and the value of K is significantly lower in PCa compared to BPH and normal tissue. In their systematic and meta-analysis article, Brancato *et al*. stated that D_K, K, and D_{IVIM} parameters are probably helpful in PCa diagnosis, but f and D* parameters have no effective usefulness.[39] Therefore, according to the studies, among parameters of the DKI, IVIM, and ADC, it seems that ADC, D_k, D_{IVIM}, and K are the most important, which can be used as an indicator to distinguish PCa from normal tissue.

In this study, for DKI and IVIM, the AUC values in the detection of PCa were accessed at 0.94 and 0.79, respectively. The sensitivity and specificity of D_K and K for PCa grading were the same 96% (95% CI 89%–98%) and 83% (95% CI 77%–87%), respectively. In a meta-analysis study using 19 articles, the AUC value obtained for DWI in the PCa detection was equal to 0.85.[40] Another study using 21 articles mentioned a value of 0.9.[41] In a meta-analysis study aimed at investigating the diagnostic performance of DKI parameters in breast cancer grading, sensitivity and specificity values were obtained for K (90% and 88%), D (86% and 88%), and ADC (85% and 83%).[42] Wang *et al*., in a review study, assessed the diagnostic performance of ADC, DKI, and IVIM parameters for differentiating benign and malignant nonfatty musculoskeletal soft-tissue tumors. Thirteen ADC studies showed the AUC value for ADC was 0.806. Four IVIM studies calculated the AUC values for D_{IVIM} 0.874, D* 0.736, and f 0.573. Two DKI studies stated the AUC value of K at 0.97 and 0.89.[43]

In general, the DKI model probably has a higher ability to detect PCa from normal tissue than the IVIM model and the same diagnostic performance compared to DWI and ADC.

The reasons for this superiority or the same diagnostic performance should be found in the DKI model features compared with other models. The DWI measures the microscopic movement of water molecules in the extracellular space. Due to more water restriction, the amount of ADC decreases in tumor tissue. The diffusion of water around the cancerous lesion is restricted due to the density of the tumor tissue, and ADC cannot fully record diffusion inhomogeneity within the tumor voxel.[44] However, the kurtosis model can show this variation. In fact, in the DKI method, it is assumed that the movement of water has a non-Gaussian distribution due to the complex structure and heterogeneity of tissues.[45] The IVIM model considers both diffusion components, assuming a Gaussian distribution and perfusion, providing quantitative information about the microstructure and microvasculature.[46,47]

Two limitations may affect the reliability of our findings. Data may be missing because we only included studies written in English. Another limitation is that several articles whose title was about one of the types of diffusion were not entirely free and did not have enough information in the abstract were excluded from our study. There is insufficient certainty that they were eligible for inclusion in our study.

CONCLUSION

According to the studies, among the DKI, IVIM, and ADC parameters, it seems that ADC, D_k, D_{IVIM}, and K are the most important, which can be used as an indicator to distinguish PCa from normal tissue. In general, the DKI model probably has a higher ability to detect PCa from normal tissue than the IVIM model. DKI probably has the same diagnostic performance in PCa detection and grading compared to DWI and ADC, so it is not recommended to be used routinely in clinical evaluation and, therefore, multiparametric techniques.

Author contributions

Conceptualization, HN, DSG, MRM, MM; Methodology: HN, DSG, MRM, MM; Validation: DSG, HN; Investigation: HN, DSG, MRM, MM; Resources: MM, DSG; Review and Editing: MRM, DSG; Supervision: MM, DSG; Project Administration: MM; Funding Acquisition:MM; All authors have read and agreed to the published version of the manuscript.

Institutional review board statement

This article does not contain any studies with human participants or animals performed by any of the authors.

Data availability statement

The data presented in this study are available on request from the corresponding author.

Financial support and sponsorship

This study was financially supported by Isfahan University of Medical Sciences, Isfahan, Iran (grant number 3400544).

Conflicts of interest

There are no conflicts of interest.

REFERENCES

1. Siegel RL, Miller KD, Fedewa SA, Ahnen DJ, Meester RG, Barzi A, *et al.* Colorectal cancer statistics, 2017. CA Cancer J Clin 2017;67:177-93.
2. Welch HG, Black WC. Overdiagnosis in cancer. J Natl Cancer Inst 2010;102:605-13.
3. Hegde JV, Mulkern RV, Panych LP, Fennessy FM, Fedorov A, Maier SE, *et al.* Multiparametric MRI of prostate cancer: An update on state-of-the-art techniques and their performance in detecting and localizing prostate cancer. J Magn Reson Imaging 2013;37:1035-54.
4. de Rooij M, Hamoen EH, Fütterer JJ, Barentsz JO, Rovers MM. Accuracy of multiparametric MRI for prostate cancer detection: A meta-analysis. AJR Am J Roentgenol 2014;202:343-51.
5. Fütterer JJ, Briganti A, De Visschere P, Emberton M, Giannarini G, Kirkham A, *et al.* Can clinically significant prostate cancer be detected with multiparametric magnetic resonance imaging? A systematic review of the literature. Eur Urol 2015;68:1045-53.
6. Di Minno A, Aveta A, Gelzo M, Tripodi L, Pandolfo SD, Crocetto F, *et al.* 8-hydroxy-2-deoxyguanosine and 8-iso-prostaglandin F2α: Putative biomarkers to assess oxidative stress damage following robot-assisted radical prostatectomy (RARP). J Clin Med 2022;11:6102.
7. Fusco R, Sansone M, Granata V, Setola SV, Petrillo A. A systematic review on multiparametric MR imaging in prostate cancer detection. Infect Agent Cancer 2017;12:57.
8. Zhu G, Luo J, Ouyang Z, Cheng Z, Deng Y, Guan Y, *et al.* The assessment of prostate cancer aggressiveness using a combination of quantitative diffusion-weighted imaging and dynamic contrast-enhanced magnetic resonance imaging. Cancer Manag Res 2021;13:5287-95.
9. Johnson LM, Turkbey B, Figg WD, Choyke PL. Multiparametric MRI in prostate cancer management. Nat Rev Clin Oncol 2014;11:346-53.
10. Barentsz JO, Richenberg J, Clements R, Choyke P, Verma S, Villeirs G, *et al.* ESUR prostate MR guidelines 2012. Eur Radiol 2012;22:746-57.
11. Iima M, Honda M, Sigmund EE, Ohno Kishimoto A, Kataoka M, Togashi K. Diffusion MRI of the breast: Current status and future directions. J Magn Reson Imaging 2020;52:70-90.
12. Monti S, Brancato V, Di Costanzo G, Basso L, Puglia M, Ragozzino A, *et al.* Multiparametric MRI for prostate cancer detection: New insights into the combined use of a radiomic approach with advanced acquisition protocol. Cancers (Basel) 2020;12:390.
13. Vargas HA, Lawrence EM, Mazaheri Y, Sala E. Updates in advanced diffusion-weighted magnetic resonance imaging techniques in the evaluation of prostate cancer. World J Radiol 2015;7:184-8.
14. Liu Y, Wang X, Cui Y, Jiang Y, Yu L, Liu M, *et al.* Comparative study of monoexponential, intravoxel incoherent motion, kurtosis, and IVIM-kurtosis models for the diagnosis and aggressiveness assessment of prostate cancer. Front Oncol 2020;10:1763.
15. Tian W, Zhang J, Tian F, Shen J, Niu T, He G, *et al.* Correlation of diffusion tensor imaging parameters and Gleason scores of prostate cancer. Exp Ther Med 2018;15:351-6.
16. Choi YJ, Kim JK, Kim N, Kim KW, Choi EK, Cho KS. Functional MR imaging of prostate cancer. Radiographics 2007;27:63-75.
17. Moher D, Liberati A, Tetzlaff J, Altman DG, PRISMA Group. Preferred Reporting Items for Systematic Reviews and Meta-analyses: The PRISMA statement. Int J Surg 2010;8:336-41.
18. Akamine Y, Ueda Y, Ueno Y, Sofue K, Murakami T, Yoneyama M, *et al.* Application of hierarchical clustering to multi-parametric MR in prostate: Differentiation of tumor and normal tissue with high accuracy. Magn Reson Imaging 2020;74:90-5.
19. Barrett T, McLean M, Priest AN, Lawrence EM, Patterson AJ, Koo BC, *et al.* Diagnostic evaluation of magnetization transfer and diffusion kurtosis imaging for prostate cancer detection in a re-biopsy population. Eur Radiol 2018;28:3141-50.
20. Li C, Yu L, Jiang Y, Cui Y, Liu Y, Shi K, *et al.* The histogram analysis of intravoxel incoherent motion-kurtosis model in the diagnosis and grading of prostate cancer – A preliminary study. Front Oncol 2021;11:604428.
21. Tamada T, Prabhu V, Li J, Babb JS, Taneja SS, Rosenkrantz AB. Prostate cancer: Diffusion-weighted MR imaging for detection and assessment of aggressiveness-comparison between conventional and kurtosis models. Radiology 2017;284:100-8.
22. Tamura C, Shinmoto H, Soga S, Okamura T, Sato H, Okuaki T, *et al.* Diffusion kurtosis imaging study of prostate cancer: Preliminary findings. J Magn Reson Imaging 2014;40:723-9.
23. Wang Q, Li H, Yan X, Wu CJ, Liu XS, Shi HB, *et al.*, editors. Histogram analysis of diffusion kurtosis magnetic resonance imaging in differentiation of pathologic Gleason grade of prostate cancer. In: Urol Oncol Semin Orig Invest 2015;33: 337.e15-337.e24.
24. Wang X, Tu N, Qin T, Xing F, Wang P, Wu G. Diffusion kurtosis imaging combined with DWI at 3-T MRI for detection and assessment of aggressiveness of prostate cancer. AJR Am J Roentgenol 2018;211:797-804.
25. Yin H, Wang D, Yan R, Jin X, Hu Y, Zhai Z, *et al.* Comparison of diffusion kurtosis imaging and amide proton transfer imaging in the diagnosis and risk assessment of prostate cancer. Front Oncol 2021;11:640906.
26. Park H, Kim SH, Lee Y, Son JH. Comparison of diagnostic performance between diffusion kurtosis imaging parameters and mono-exponential ADC for determination of clinically significant cancer in patients with prostate cancer. Abdom Radiol (NY) 2020;45:4235-43.
27. Chen YJ, Pu YS, Chueh SC, Shun CT, Chu WC, Tseng WY. Diffusion MRI predicts transrectal ultrasound biopsy results in prostate cancer detection. J Magn Reson Imaging 2011;33:356-63.
28. Kozlowski P, Chang SD, Jones EC, Goldenberg SL. Assessment of the need for DCE MRI in the detection of dominant lesions in the whole gland: Correlation between histology and MRI of prostate cancer. NMR Biomed 2018;31:e3882. [doi: 10.1002/nbm.3882].
29. Kozlowski P, Chang SD, Meng R, Mädler B, Bell R, Jones EC, *et al.* Combined prostate diffusion tensor imaging and dynamic contrast enhanced MRI at 3T – Quantitative correlation with biopsy. Magn Reson Imaging 2010;28:621-8.
30. Li C, Chen M, Li S, Zhao X, Zhang C, Luo X, *et al.* Detection of prostate cancer in peripheral zone: Comparison of MR diffusion tensor imaging, quantitative dynamic contrast-enhanced MRI, and the two techniques combined at 3.0 T. Acta Radiol 2014;55:239-47.
31. Bao J, Wang X, Hu C, Hou J, Dong F, Guo L. Differentiation of prostate cancer lesions in the transition zone by diffusion-weighted MRI. Eur J Radiol Open 2017;4:123-8.
32. Barbieri S, Brönnimann M, Boxler S, Vermathen P, Thoeny HC. Differentiation of prostate cancer lesions with high and with low Gleason score by diffusion-weighted MRI. Eur Radiol 2017;27:1547-55.

33. Lee CC, Chang KH, Chiu FM, Ou YC, Hwang JI, Hsueh KC, *et al*. Using IVIM parameters to differentiate prostate cancer and contralateral normal tissue through fusion of MRI images with whole-mount pathology specimen images by control point registration method. Diagnostics (Basel) 2021;11:2340.
34. Valerio M, Zini C, Fierro D, Giura F, Colarieti A, Giuliani A, *et al.* 3T multiparametric MRI of the prostate: Does intravoxel incoherent motion diffusion imaging have a role in the detection and stratification of prostate cancer in the peripheral zone? Eur J Radiol 2016;85:790-4.
35. Nematollahi H, Moslehi M, Aminolroayaei F, Maleki M, Shahbazi Gahrouei D. Diagnostic performance evaluation of multiparametric magnetic resonance imaging in the detection of prostate cancer with supervised machine learning methods. Diagnostics (Basel) 2023;13:806.
36. Lee H, Hwang SI, Lee HJ, Byun SS, Lee SE, Hong SK. Diagnostic performance of diffusion-weighted imaging for prostate cancer: Peripheral zone versus transition zone. PLoS One 2018;13:e0199636.
37. He N, Li Z, Li X, Dai W, Peng C, Wu Y, *et al.* Intravoxel incoherent motion diffusion-weighted imaging used to detect prostate cancer and stratify tumor grade: A meta-analysis. Front Oncol 2020;10:1623.
38. Si Y, Liu RB. Diagnostic performance of monoexponential DWI versus diffusion kurtosis imaging in prostate cancer: A systematic review and meta-analysis. AJR Am J Roentgenol 2018;211:358-68.
39. Brancato V, Cavaliere C, Salvatore M, Monti S. Non-Gaussian models of diffusion weighted imaging for detection and characterization of prostate cancer: A systematic review and meta-analysis. Sci Rep 2019;9:16837.
40. Tan CH, Wei W, Johnson V, Kundra V. Diffusion-weighted MRI in the detection of prostate cancer: Meta-analysis. AJR Am J Roentgenol 2012;199:822-9.
41. Jie C, Rongbo L, Ping T. The value of diffusion-weighted imaging in the detection of prostate cancer: A meta-analysis. Eur Radiol 2014;24:1929-41.
42. Li Z, Li X, Peng C, Dai W, Huang H, Li X, *et al.* The diagnostic performance of diffusion kurtosis imaging in the characterization of breast tumors: A meta-analysis. Front Oncol 2020;10:575272.
43. Wang Q, Xiao X, Liang Y, Wen H, Wen X, Gu M, *et al.* Diagnostic performance of diffusion MRI for differentiating benign and malignant non fatty musculoskeletal soft tissue tumors: A systematic review and meta-analysis. J Cancer 2021;12:7399-412.
44. Wang F, Wang Y, Zhou Y, Liu C, Xie L, Zhou Z, *et al.* Comparison between types I and II epithelial ovarian cancer using histogram analysis of monoexponential, biexponential, and stretched-exponential diffusion models. J Magn Reson Imaging 2017;46:1797-809.
45. Jensen JH, Helpern JA, Ramani A, Lu H, Kaczynski K. Diffusional kurtosis imaging: The quantification of non-Gaussian water diffusion by means of magnetic resonance imaging. Magn Reson Med 2005;53:1432-40.
46. Malagi AV, Netaji A, Kumar V, Baidya Kayal E, Khare K, Das CJ, *et al.* IVIM-DKI for differentiation between prostate cancer and benign prostatic hyperplasia: Comparison of 1.5 T versus 3 T MRI. MAGMA 2022;35:609-20.
47. Le Bihan D, Breton E, Lallemand D, Aubin ML, Vignaud J, Laval Jeantet M. Separation of diffusion and perfusion in intravoxel incoherent motion MR imaging. Radiology 1988;168:497-505.